Antiviral Research 170 (2019) 104565

Contents lists available at ScienceDirect

Antiviral Research

journal homepage: www.elsevier.com/locate/antiviral

Susceptibility of Enterovirus-D68 to RNAi-mediated antiviral knockdown

Nicholas Klaiber, Michael A. McVoy, Wei Zhao*

Department of Pediatrics, Virginia Commonwealth University, Richmond, VA, USA

ARTICLE INFO

Keywords:
RNA interference
Enterovirus-D68
Antivirals
RNA-dependent RNA polymerase
bronchiolitis

ABSTRACT

Enterovirus D68 (EV-D68) represents an emerging pathogen which has demonstrated a capacity for causing epidemic illness in pediatric and immunocompromised patients. With no effective antiviral treatment available, therapeutic interventions are currently limited to supportive care. Utilizing available genomic sequences from the 2014 B3 Epidemic EV-D68 clade and the 1962 Fermon EV-D68 strains, we performed *in silico* comparative genomic analysis, identifying several islands of phylogenetic conservation within the viral RNA-dependent RNA polymerase gene. The effects of transfecting short-interfering double-stranded RNA (siRNA) molecules targeting these conserved sequences were tested *in vitro* using a human rhabdomyosarcoma cell-based model of EV-D68 infection. Two siRNA sequences demonstrated reproducible ability to abrogate EV-D68-mediated cytopathic effect *in vitro*. These siRNA sequences were also able to decrease EV-D68 genome replication, VP-2 capsid protein expression, and infectious particle production *in vitro*. EV-D68 knockdown was sequence-specific and not observed in cells treated with a negative control siRNA lacking sequence homology to the viral genome. The regions targeted by these siRNA's are located in highly conserved regions of the RNA-dependent RNA polymerase gene. The most potent siRNA targeted a sequence found in subsequent enzyme crystallographic studies to enhance the enzyme's thermostability (Wang et al., 2017). Topical nebulized siRNAs have recently been utilized as antivirals in human studies, with no adverse effects or toxicities noted (Gottlieb et al., 2016). Sequence selection is likely one primary factor determining the potential efficacy of such therapeutics. These results demonstrate that the identified siRNA sequences are able to suppress EV-D68 replication and cytopathic effect *in vitro*.

Picornaviruses represent one of the most common causes of acute illness in human populations across the globe. They also contribute significantly to the worldwide disease burden of asthma and can lead to chronic infection in immunocompromised hosts. Enterovirus D68 (EV-D68), formerly classified as rhinovirus 87, was responsible for an epidemic of pediatric respiratory illness that spread throughout North America during 2014. This was the largest outbreak of EV-D68 yet documented, with 1153 confirmed cases and 17 deaths (Messacar et al., 2016). The CDC estimates that millions of children were likely infected, though only a fraction of these ultimately had diagnostic testing performed during 2014. Global surveillance data indicate that over the last decade there has been an increase in EV-D68 infection rates concurrent with increasing viral genome polymorphism (Gong et al., 2016). Between 2000 and 2010 large outbreaks of EV-D68 infection were documented in the Philippines, Asia, Africa, and Europe (Rahamat-Langendoen et al., 2011, Imamura and Oshitani, 2015 and Holm-Hansen et al., 2016).

RNA interference (RNAi) is a highly conserved cellular pathway present in eukaryotic cells (Hannon, 2002) most frequently utilized for interrogating gene function. The capability of siRNAs to knockdown viral genes has also been documented (Liu et al., 2016). RNAi is notable for both its remarkable specificity (a single nucleotide mismatch between the guide and target can abolish silencing) and robustness, with decreases in endogenous protein expression approaching 90% commonly achieved during *in vitro* transfections of permissive cell lines (Ambesajir et al., 2012). Human trials of a nebulized siRNA-based treatment for respiratory syncytial virus infection have demonstrated safety in lung transplant patients with an associated decrease in bronchiolitis obliterans, though more work remains to optimize efficacy (Gottlieb et al., 2016). Previously it has been shown that rhinovirus 1B, 16, and enterovirus 71 are susceptible to *in vitro* RNAi-mediated suppression (Phipps et al., 2004; Wu et al., 2009). Like these picornaviruses, EV-D68 possess a single-stranded positive sense RNA genome that undergoes replication and accumulation within the cytoplasm of infected cells, leaving it potentially vulnerable to degradation by the RISC.

We performed comparative genomic analysis examining the Fermon and 2014 B3 clade epidemic US/MO/2014 strain of EV-D68, which revealed several regions of extensive sequence conservation within the RNA-dependent RNA polymerase (RdRP) gene. Three siRNAs targeting

* Corresponding author. PO Box 980225, Department of Pediatrics, 1000 E Broad Street, Richmond, VA. 23298-0225, USA.
E-mail address: wei.zhao@vcuhealth.org (W. Zhao).

https://doi.org/10.1016/j.antiviral.2019.104565
Received 29 May 2019; Received in revised form 17 July 2019; Accepted 20 July 2019
Available online 20 July 2019
0166-3542/

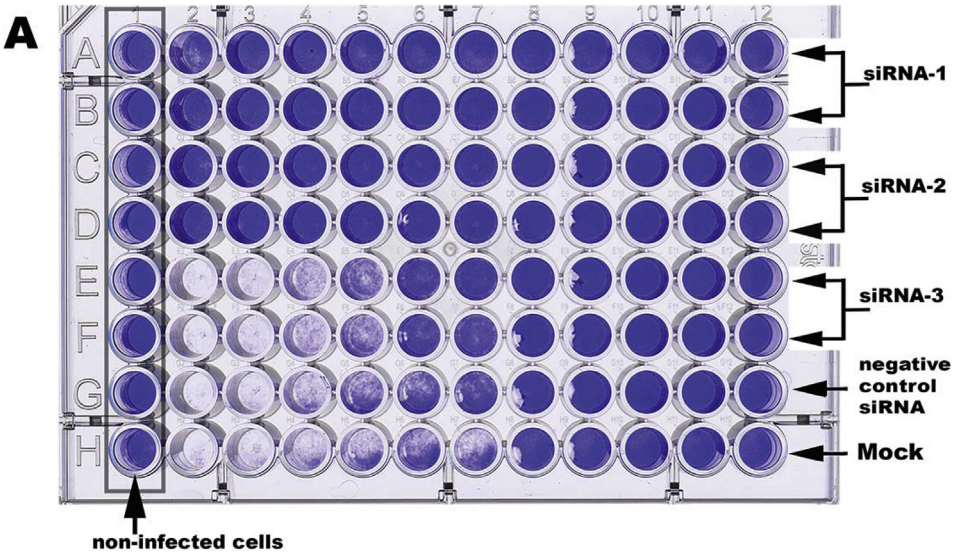

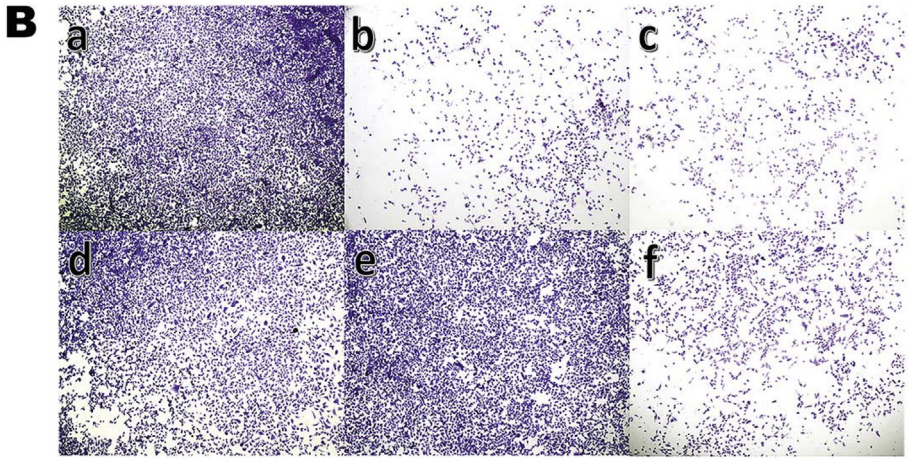

Fig. 1. Effects of siRNA transfection on EV-D68 CPE. (A) RD cell monolayers in a 96-well plate were mock-transfected or transfected with siRNAs. After 24 h cells were infected with EV-D68 strain US/MO/2014, then incubated for five days prior to staining with crystal violet. Column 1 contains non-infected control cells; column 2 contains cells infected with EV-D68 at an MOI of 2.8; columns 3–12 were infected with 10-fold serial dilutions of the EV-D68 inoculum used in column 2. 24 h prior to infection, rows were transfected with 10 nM siRNA-1 (rows A and B), siRNA-2 (rows C and D), siRNA-3 (rows E and F), negative control siRNA (row G), or mock-transfected (row H). **(B)** Representative 40× micrographs from wells of the 96-well plate shown in panel A. **a.** well A1 (non-infected cells); **b.** well H2 (no siRNA); **c.** well G2 (negative control siRNA); **d.** well A2 (siRNA-1)**; e.** well C2 (siRNA-2); **f.** well E2 (siRNA-3).

these islands of phylogenetic conservation (supplementary data) were synthesized (IDT) and tested *in vitro* using a human rhabdomyosarcoma cell (RD cells ATCC® CCL-136) based model of EV-D68 infection. RNAi max transfection reagent (Invitrogen) was utilized to facilitate transfection of all siRNAs. Data were subjected to ANOVA one-way analysis using Prism 5 software (GraphPad Software, La Jolla, CA, USA) to determine the significance of variability between groups. The $2^{\Delta Ct}$ method was utilized to calculate relative copy numbers in RT-PCR experiments.

RD cells that were transfected with siRNA-1 or siRNA-2, 24 h prior to infection with EV-D68 (US/MO/2014 ATCC VR-1823), showed no CPE at 5 days post infection. When stained with crystal violet (Fig. 1A), and examined under a light microscope (Fig. 1B), cells were identical to non-infected controls. In contrast, wells that were mock transfected, transfected with siRNA-3, or transfected with the negative control siRNA prior to infection showed prominent CPE at five days post-infection. Transfection with both siRNA-1 and siRNA-2 abrogated the capacity of a 2.1×10^8 tissue culture 50% infectious dose ($TCID_{50}$)/ml viral stock solution to produce any detectable CPE. $TCID_{50}$ was calculated by the Spearman & Kärber method (Wulff et al., 2012).

Following staining with crystal violet absorbance at 570 nm was used to quantify remaining cells. In wells transfected with siRNA-1 or siRNA-2, there was no statistically significant difference in absorption when compared with non-infected control wells. Absorbance was significantly decreased in wells transfected with siRNA-3, negative control siRNAs, or mock transfected wells 5 days after infection with EV-D68 (Fig. 2A).

To further quantify cytopathic effect, cells were stained with Hoechst and the fluorescence in each well was measured using 361/497 nm excitation/emission settings. Similar to the absorbance data, wells treated with siRNA-1 and siRNA-2 prior to infection, showed no statistically significant difference in fluorescence when compared to non-infected controls (Fig. 2B). Infected wells that had been mock transfected, transfected with siRNA-3, or transfected with negative control siRNA prior to infection, showed significantly decreased fluorescence when compared to non-infected wells. When the concentrations of siRNA-1 or siRNA-2 were varied, dose-dependent escalation of their protective effects was noted with EC_{50} concentrations of 15 nM and 16 nM, respectively (Fig. 2C).

To determine the impact of siRNA treatment on EV-D68 genome replication, RT-PCR was used to quantitate genome copy number five days after infection (Wylie et al., 2015). Transfection with siRNA-1 or siRNA-2 at 10 nM significantly decreased EV-D68 genome copy number when compared to wells transfected with siRNA 3, negative control siRNA, or the mock transfected controls ($p < 0.001$) (Fig. 3A). Transfection with siRNA-1 or siRNA-2 produced 16- or 26-fold reductions in EV-D68 genome copy numbers, respectively (Fig. 3B).

Due to the fact that genome copy number may not always accurately reflect picornavirus infectious particle titers, RD cell monolayers were exposed to serial dilutions of culture media collected five days after infection from 96 well plates. Culture media from infected wells transfected with siRNA-1 or siRNA-2 showed decreased titers of infectious particles compared to culture media harvested from siRNA-3-

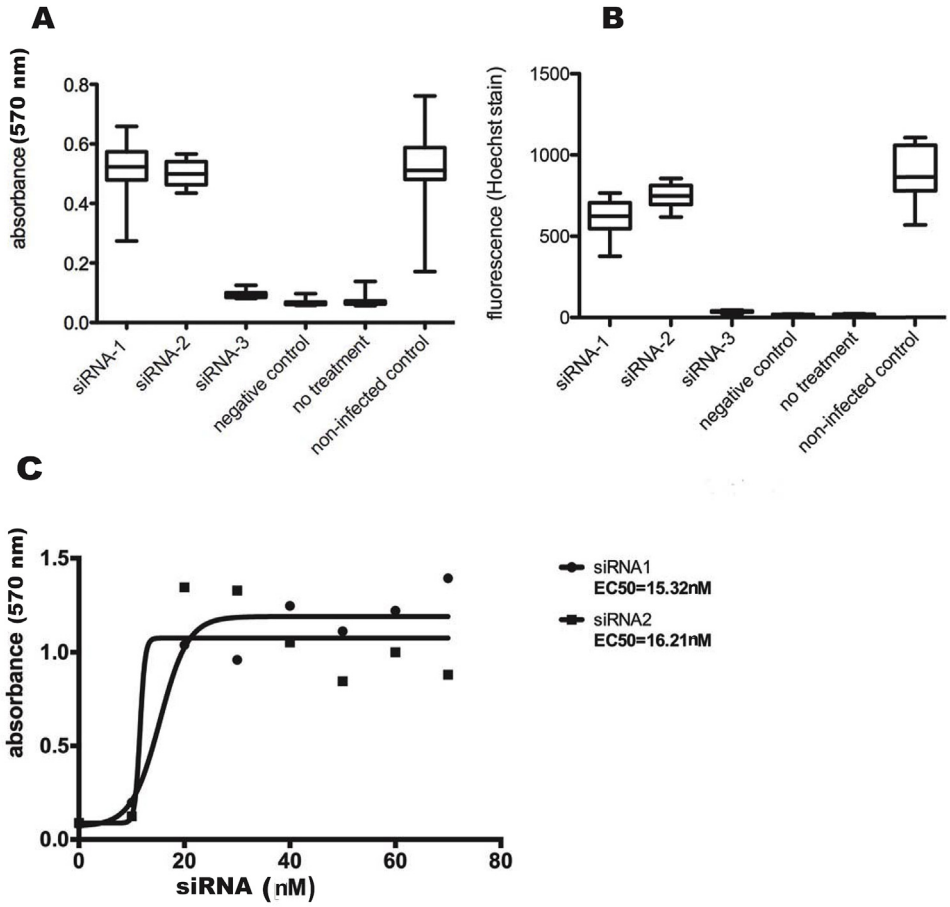

Fig. 2. Effects of siRNA transfection on cell survival five days post-infection with EV-D68. (A) Crystal violet staining was quantitated by measuring the OD 570 nm for each well of the plate shown in Fig. 1A. The data shown are for cells that were either non-infected or infected with an MOI of 2.8. There was a statistically significant increase in absorbance ($p < 0.0001$) in cells treated with siRNA1 or siRNA2 compared with controls. **(B)** A replicate experiment to that shown in Fig. 1 was stained with Hoechst stain instead of crystal violet and fluorescence was subsequently quantified and compared between transfected and non-transfected groups. **(C)** RD cell monolayers in a 96-well plate were transfected with increasing final concentrations of siRNA from 5 nM to 70 nM and then infected 24 h later with EV-D68 at an MOI of 2.8. After incubation for five days wells were stained with crystal violet. Absorbance at 570 nm was measured and plotted against log siRNA concentration and EC_{50} values were calculated as the inflection points of best-fit four-parameter curves.

or negative control siRNA-treated wells (Fig. 3C). CPE was not evident in wells inoculated with culture media from wells treated with siRNA-1 beyond the 10^{-2} dilution or with culture media from wells treated with siRNA-2 beyond the 10^{-1} dilution. In contrast, CPE was visible in monolayers inoculated with all (10^{-2} to 10^{-5}) dilutions of culture media from siRNA-3- or negative control siRNA-treated wells (Fig. 3C). Thus, treatment with siRNA-1 or siRNA-2 reduced production of infectious EV-D68 by two and three logs respectively.

To determine if siRNA transfection was capable of inhibiting viral protein expression, cells were stained with EV-D68 VP2 antibodies (Genetex) 48 h after infection. The results revealed a decrease in EV-D68 VP2 protein in cells transfected with siRNA-1 or siRNA-2 to levels similar to non-infected controls (Fig. 4). In contrast, cells transfected with siRNA-3, negative control siRNA, or mock transfected cells showed abundant expression of EV-D68 VP2 protein (Fig. 4).

Our data demonstrates that EV-D68 is susceptible to knockdown via the RNAi pathway. EV-D68 phylogeny currently designates four major subtypes of the virus denoted A, B, C, and D (Tan et al., 2015). Each of these contains multiple subclades. During the 2014 North American EV-D68 epidemic, comprehensive genomic sequencing efforts revealed the emergence of multiple new clades (Du et al., 2015). Subsequently in 2016, 159 samples from the Lower Hudson River valley tested positive for EV-D68 during the summer of 2016 which sequencing revealed was linked to the subclade B3 (Huang et al., 2016; C. Wang et al., 2017; G. Wang et al., 2017).

Several point mutations identified in the 2014 EV-D68 B1 clade were noted surrounding cleavage sites utilized by the viral $2A^{pro}$ and $3C^{pro}$ enzyme (Huang et al., 2015). It was hypothesized that these mutations might confer increased viral replicative capacity upon the resulting virus. Our unpublished data supports this conjecture that the 2014 epidemic EV-D68 strain does indeed replicate at a greater rate than the Fermon strain *in vitro,* though this has yet to be confirmed with *in vivo* analyses.

Though the Fermon and 2014 epidemic strains of EV-D68 have greater than 88% overall homology, we observed that stretches of exact sequence conservation greater than 50 base pairs long were present but rare. Taking advantage of this we were able to design siRNAs with potent anti-viral activity against EV-D68. Two of the three siRNAs were observed to provide potent suppression of EV-D68 CPE, viral genome replication, viral protein expression, and infectious particle production. Antiviral activity varied depending upon the sequence of the siRNA transfected. A single non-conserved nucleotide which is present in the Fermon strain, but which is not ubiquitous in more recent epidemic strains (including US/MO/2014) was incorporated in to siRNA-3 (Table 1). This siRNA did not produce any measurable effect on EV-D68 CPE or replication of either the Fermon (data not shown) or the US/MO/2014 EV-D68 strains, highlighting the importance of appropriate target selection to achieve antiviral activity.

Subsequent to the completion of the experiments described here within, a crystal structure of the EV-D68 RdRP was published (C. Wang et al., 2017; G. Wang et al., 2017). This data revealed that, similar to other picornaviruses, the EV-D68 RdRP structurally resembles a cupped right hand. The sequence of siRNA-2, which showed the highest level of antiviral activity, targets the extremely conserved nucleotide channel formed by the index finger and thumb of the RdRP. The amino acids 391 through 399 of the EV-D68 RdRP, which are encoded by the viral genome sequences homologous to siRNA-2, interact with amino acids at the N-terminus of the polymerase to stabilize the molecule. Mutations introduced to this region decreased the thermostability of the EV-D68 RdRP (C. Wang et al., 2017; G. Wang et al., 2017). siRNA-1 targets the amino acids 447–455 of the RdRP directly adjacent to the 3′ UTR. These amino acids are conserved but were not observed to have any protein

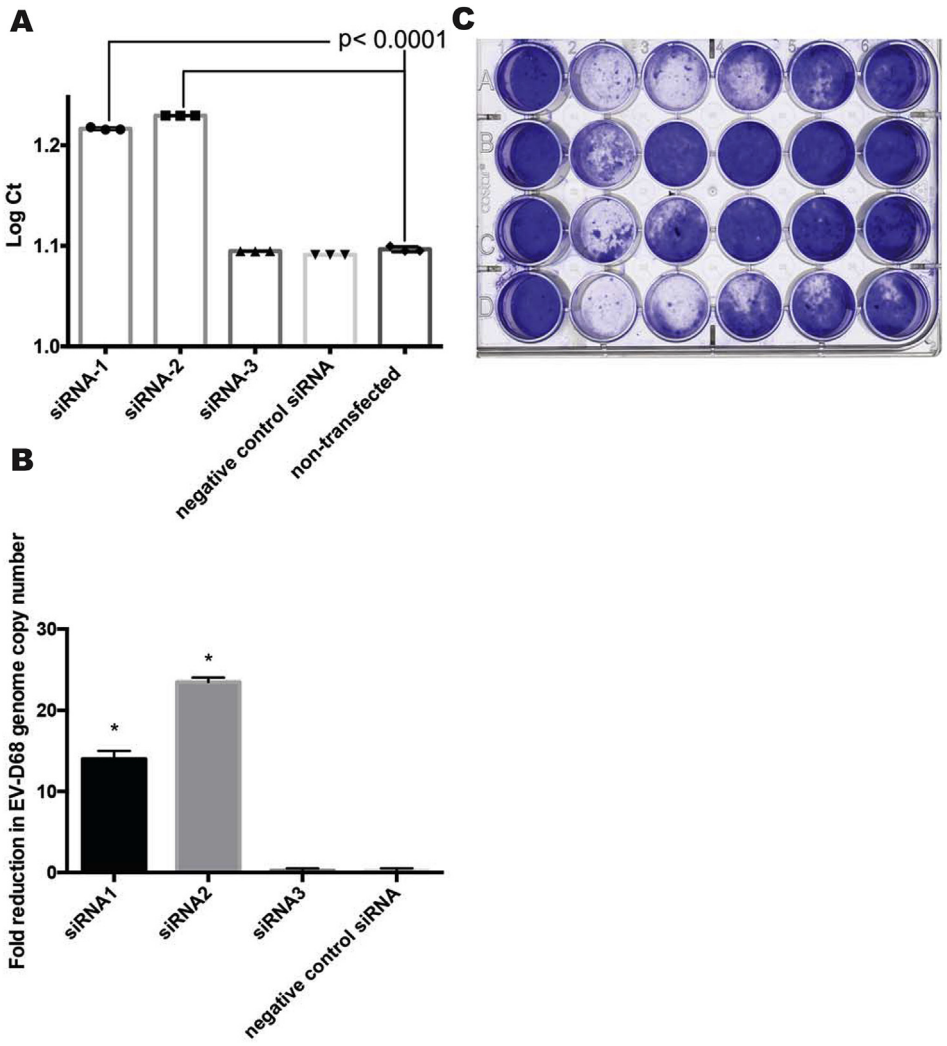

Fig. 3. Effects of siRNA transfection on EV-D68 genome copy number and infectious virus yield five days post-infection. (A) RD cell monolayers in a 96-well plate were mock transfected or transfected with 10 nM siRNAs and 24 h later infected with EV-D68 US/MO/2014 at an MOI of 2.8. After incubation for five days RNA was isolated and EV-D68 genomes were quantitated by RT-PCR. Results were expressed as mean cycle threshold (Ct) values. **(B)** data from 3A were normalized to show fold reduction in EV-D68 genome copy number ($*p < 0.001$). **(C)** Culture media from the individual wells described in panel A were 10-fold serially diluted and added to fresh RD cell monolayers in a 24-well plate. After incubation for five days the wells were stained with crystal violet. Wells in column 1 were mock-treated (non-infected). Wells in columns 2 to 6 were inoculated with culture media diluted 10^{-1} to 10^{-5}, respectively, derived from infected wells treated with siRNA-3 (row A), siRNA-2 (row B), siRNA-1 (row C), or negative control siRNA (row D).

stabilizing motifs in the aforementioned crystallographic study. Such motifs represent an attractive target for a therapy so dependent upon sequence specificity as RNAi due to the reduced potential for viable infectious particles with mutations conferring resistance. siRNA-3 targets the nucleotides encoding residues 31–39, which are directly adjacent to amino acids 1–30 of the RdRP. While amino acids 1–30 form the highly conserved motif noted to structurally interact with the thumb region stabilizing the polymerase, residues 31–39 (targeted by siRNA-3) do not form any motifs noted to be structurally critical by the x-ray crystallography data (C. Wang et al., 2017; G. Wang et al., 2017).

The ability of siRNAs to result in antiviral activity is dependent upon the secondary structure of the target RNA sequence and the secondary structure itself can be functional (*i.e.*, via interactions with host cellular machinery), resulting in evolutionary preservation of these

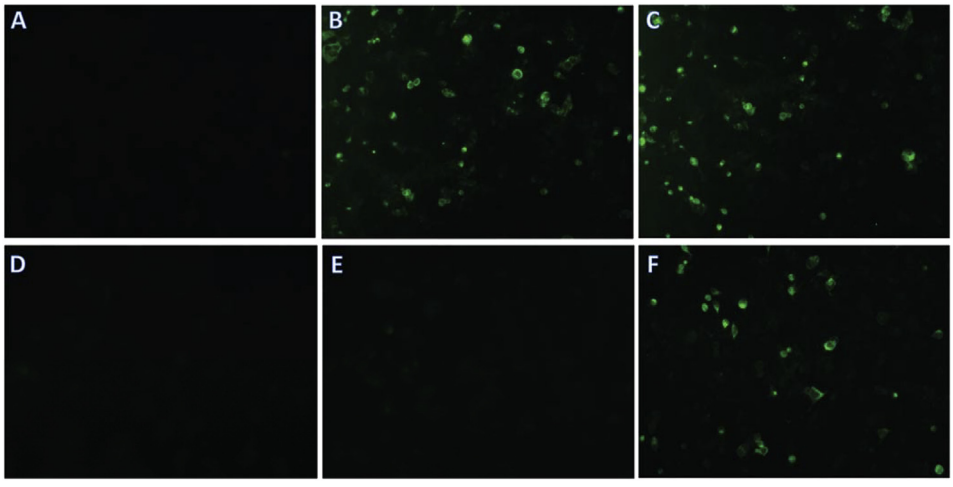

Fig. 4. Effects of siRNA transfection on EV-D68 VP2 protein expression. RD cell monolayers were mock transfected or transfected with 10 nM siRNA solution and 24 h later mock infected or infected with EV-D68 US/MO/2014 at an MOI of 2.8. After incubation for 48 h the cells were fixed and stained for EV-D68 VP2 protein using indirect immunofluorescence. (A) mock-infected; (B–F) infected and treated with (B) no siRNA (transfection agent only), (C) negative control siRNA, (D) siRNA1, (E) siRNA2, (F) siRNA3.

nucleotide sequences. The 5′ untranslated region (UTR) of picornaviruses serves as an example of such an effect. Previous experiments revealed that siRNA's targeting this region did not result in antiviral activity against rhinovirus *in vitro* (10). This is likely attributable to the complex cloverleaf secondary structure of the viral genome in this region limiting access of the RISC to the target. Due to this observation we did not attempt to target the EV-D68 5′ UTR despite its high level of interspecies conservation. These same experiments did note antiviral activity from an siRNA targeting a genomic region encoding the rhinovirus RdRP around a highly conserved aspartic acid residue (Phipps et al., 2004). Any viable siRNA-based antiviral will likely need to target multiple viral sequences simultaneously, with each target having both secondary structures accessible to the RISC and sequences of high phylogenetic conservation.

Delivery has been a primary obstacle to effective RNAi-based therapeutics. The respiratory epithelium offers the potential for circumventing this technical hindrance due to its anatomical location and the apparent amenability of the epithelium to RNAi uptake. Our unpublished animal data suggest that *in vivo* knockdown of EV-D68 is possible at the nasal epithelium with topical siRNA application. Preliminary human trials have also provided proof-of-principle that nebulized delivery of siRNAs is feasible (Gottlieb et al., 2016). In 2018 the FDA approved the first siRNA based drug, Patisiran, to treat hereditary transthyretin amyloidosis (Adams et al., 2018). Picornaviruses, due both to their genomic material, lifecycles, and sites of infection, may represent a feasible target for RNAi-based therapeutics with efficacy predicated upon appropriate sequence selection.

Funding

This work was supported by Grant from Children's Hospital Foundation and CCTR Endowment Fund of Virginia Commonwealth University.

Appendix A. Supplementary data

Supplementary data to this article can be found online at https://doi.org/10.1016/j.antiviral.2019.104565.

References

Adams, D., Gonzalez-Duarte, A., O'Riordan, W.D., Yang, C.C., Ueda, M., et al., 2018. Patisiran, an RNAi therapeutic, for hereditary transthyretin amyloidosis. N. Engl. J. Med. 379, 11–21.

Ambesajir, A., Kaushik, A., Kaushik, J.J., Petros, S.T., 2012. RNA interference: a futuristic tool and its therapeutic applications. Saudi J. Biol. Sci. 19, 395–403.

Du, J., Zheng, B., Zheng, W., Li, P., Kang, J., Hou, J., Markham, R., Zhao, K., Yu, X.F., 2015. Analysis of enterovirus 68 strains from the 2014 North American outbreak reveals a new clade. Indicating viral evolution. PLoS One 10, e0144208.

Gong, Y.N., Yang, S.L., Shih, S.R., Huang, Y.C., Chang, P.Y., Huang, C.G., Kao, K.C., Hu, H.C., Liu, Y.C., Tsao, K.C., 2016. Molecular evolution and the global reemergence of enterovirus D68 by genome-wide analysis. Medicine 95, e4416.

Gottlieb, J., Zamora, M.R., Hodges, T., Musk, A.W., Sommerwerk, U., Dilling, D., Arcasoy, S., DeVincenzo, J., Karsten, V., Shah, S., Bettencourt, B.R., Cehelsky, J., Nochur, S., Gollob, J., Vaishnaw, A., Simon, A.R., Glanville, A.R., 2016. ALN-RSV01 for prevention of bronchiolitis obliterans syndrome after respiratory syncytial virus infection in lung transplant recipients. J. Heart Lung Transplant. 35, 213–221.

Hannon, G.J., 2002. RNA interference. Nature 418, 244–251.

Holm-Hansen, C.C., Midgley, S.E., Fischer, T.K., 2016. Global emergence of enterovirus D68: a systematic review. Lancet Infect. Dis. 16, e64–e75.

Huang, W., Wang, G., Zhuge, J., Nolan, S.M., Dimitrova, N., Fallon, J.T., 2015. Whole-genome sequence analysis reveals the enterovirus D68 isolates during the United States 2014 outbreak mainly belong to a novel clade. Sci. Rep. 5, 15223.

Huang, W., Yin, C., Zhuge, J., Farooq, T., Yoon, E.C., Nolan, S.M., Chen, D., Fallon, J.T., Wang, G., 2016. Complete genome sequences of nine enterovirus D68 strains from patients of the Lower Hudson valley, New York, 2016. Genome Announc. 4, e01394–16.

Imamura, T., Oshitani, H., 2015. Global reemergence of enterovirus D68 as an important pathogen for acute respiratory infections. Rev. Med. Virol. 25, 102–114.

Liu, H., Qin, Y., Kong, Z., Shao, Q., Su, Z., Wang, S., Chen, J., 2016. siRNA targeting the 2Apro genomic region prevents enterovirus 71 replication in vitro. PLoS One 11, e0149470.

Messacar, K., Abzug, M.J., Dominguez, S.R., 2016. 2014 outbreak of enterovirus D68 in North America. J. Med. Virol. 88, 739–745.

Phipps, K.M., Martinez, A., Lu, J., Heinz, B.A., Zhao, G., 2004. Small interfering RNA molecules as potential anti-human rhinovirus agents: in vitro potency, specificity, and mechanism. Antivir. Res. 61, 49–55.

Rahamat-Langendoen, J., Riezebos-Brilman, A., Borger, R., van der Heide, R., Brandenburg, A., Scholvinck, E., Niesters, H.G., 2011. Upsurge of human enterovirus 68 infections in patients with severe respiratory tract infections. J. Clin. Virol. 52, 103–106.

Tan, Y., Hassan, F., Schuster, J.E., Simenauer, A., Selvarangan, R., Halpin, R.A., Lin, X., Fedorova, N., Stockwell, T.B., Lam, T.T., Chappell, J.D., Hartert, T.V., Holmes, E.C., Das, S.R., 2015. Molecular evolution and intraclade recombination of enterovirus D68 during the 2014 outbreak in the United States. J. Virol. 90, 1997–2007.

Wang, C., Wang, C., Li, Q., Wang, Z., Xie, W., 2017. Crystal structure and thermostability characterization of enterovirus D68 3Dpol. J. Virol. 91, e00876–17.

Wang, G., Zhuge, J., Huang, W., Nolan, S.M., Gilrane, V.L., Yin, C., Dimitrova, N., Fallon, J.T., 2017. Enterovirus D68 subclade B3 strain circulating and causing an outbreak in the United States in 2016. Sci. Rep. 7, 1242.

Wu, Z., Yang, F., Zhao, R., Zhao, L., Guo, D., Jin, Q., 2009. Identification of small interfering RNAs which inhibit the replication of several Enterovirus 71 strains in China. J. Virol. Methods 159, 233–238.

Wulff, N.H., Tzatzaris, M., Young, P.J., 2012. Monte Carlo simulation of the Spearman-Kaerber TCID50. J. Clin. Bioinform. 2. https://doi.org/10.1186/2043-9113-2-5.

Wylie, T.N., Wylie, K.M., Buller, R.S., Cannella, M., Storch, G.A., 2015. Development and evaluation of an enterovirus D68 real-time reverse transcriptase PCR assay. J. Clin. Microbiol. 53, 2641–2647.